Journal of Cancer Research and Clinical Oncology (2024) 150:421
https://doi.org/10.1007/s00432-024-05943-8

RESEARCH

The presence of cancer-associated fibroblast in breast cavity side margins is in correlation with the expression of oncoproteins by adjacent epithelial cells: a new era in cancerous potential

Zohreh Sadat Miripour[1,2] · Mina Aminifar[1] · Parisa Hoseinpour[1,3] · Fereshteh Abbasvandi[4,5] · Koosha Karimi[1] · Alireza Ghahremani[1] · Mohammad Parniani[4] · Mohammadreza Ghaderinia[1] · Faride Makiyan[1] · Parisa Aghaee[1] · Mohammad Esmaeil Akbari[5] · Mohammad Abdolahad[1,2,6]

Received: 29 June 2024 / Accepted: 4 September 2024

Abstract

Purpose Cancer-associated fibroblasts (CAFs) are one of the most critical cells in the tumor environment, with crucial roles in cancer progression and metastasis. Due to Field-Effect phenomena (also called field cancerization), the adjacent cavity side area of the margin is histologically normal, but it has been entered into neoplastic transformation due to MCT4 and MCT1 pathways activated by H_2O_2/ROS oxidative stress agents secreted by CAF in adjacent tumor bed microenvironment. This paper specifically focused on the role of cancer-associated fibroblast in breast tumor beds and its correlation with the presence of scattered cancer cells or onco-protein-activated cells (may be high risk but not completely transformed cancer cells) in the cavity side margins.

Methods In this study, the glycolytic behavior of non-tumoral cavity side margins was examined using carbon nanotube-based electrochemical biosensors integrated into a cancer diagnostic probe. This method enabled the detection of CAF accumulation sites in non-cancerous neighboring tissues of tumors, with a correlation to CAF concentration. Subsequently, RT-PCR, fluorescent, histopathological, and invasion assays were conducted on hyperglycolytic lesions to explore any correlation between the abundance of CAFs and the electrochemical responses of the non-cancerous tissues surrounding the tumor, as well as their neoplastic potential.

Results We observed overexpression of cancer-associated transcriptomes as well as the presence and hyperactivation of CAFs in cavity-side regions in which glycolytic metabolism was recorded, independent of the histopathological state of the lesion. At mean 70.4%, 66.7%, 70.4%, and 44.5% increments were observed in GLUT-1, MMP-2, N-cadherin, and MMP-9 transcriptomes by highly glycolytic but histologically cancer-free expression samples in comparison with negative controls (histologically non-cancer lesions with low glycolytic behavior).

Conclusion The presence of CAFs is correlated with the presence of high glycolytic metabolism in the cavity margin lesion, high ROS level in the lesion, and finally aggressive cancer-associated proteins (such as MMP2, …) in the margin while these metabolomes, molecules, and proteins are absent in the margins with negatively scored CDP response and low ROS level. So, it seems that when we observe CAFs in glycolytic lesions with high ROS levels, some high-risk epithelial breast cells may exist while no histological trace of cancer cells was observed. Further research on CAFs could provide valuable insights into the local recurrence of malignant breast diseases. Hence, real-time sensors can be used to detect and investigate CAFs in the non-tumoral regions surrounding tumors in cancer patients, potentially aiding in the prevention of cancer recurrence.

Keywords Cancer-associated fibroblast · Field concretization · Cavity side margin · Glycolytic behavior

Introduction

Field cancerization is one of the hot subjects recently presented in cancer biology in which CAFs play a crucial role (Chan et al. 2018; Gascard and Tlsty 2016; Martinez-Outschoorn et al. 2010; Liao et al. 2018; Vanharanta and

Zohreh Sadat Miripour and Mohammad Abdolahad contributed equally.

Koosha Karimi and Alireza Ghahremani contributed equally.

Extended author information available on the last page of the article

Published online: 17 September 2024

Massagué 2012; Gadaleta et al. 2022). The tumor stroma is no longer seen solely as physical support for mutated epithelial cells but as an essential modulator and even a driver of tumorigenicity. Within the tumor-stromal milieu, heterogeneous populations of fibroblast-like cells, collectively termed CAFs, are key players in the multicellular, stromal-dependent alterations that contribute to malignant initiation and progression (Gascard and Tlsty 2016; Giannoni et al. 2010).

High reputations of investigations are needed to reveal the correlation between the presence of CAFs in the far field from the tumor and their effect on cancer recurrences. In this phenomenon, the hydrogen peroxide and reactive oxygen species (ROS) were released by tumor-associated fibroblasts and the adjacent tumor microenvironment cells in the environment of normal stromal margins and cancerized them through "field effect" but revealed no pathological signs of cancerization (Lisanti et al. 2011).

Many methods were developed to find and indicate CAFs, such as fibroblast-cancer cell line co-cultures to investigate their markers (Martinez-Outschoorn et al. 2010; Louault et al. 2019; Erez et al. 2010) and invasive behavior of cancer cells in the presence of CAFs (Truong et al. 2019; Truong et al. 2016). Some research indicated that CAFs promoted aggressive phenotypes of breast cancer cells through epithelial-to-mesenchymal transition (EMT) induced by TGF-β1. This might be a common mechanism for acquiring metastatic potential in breast cancer cells with different biological characteristics (Yu et al. 2014). The distinct functions of CAFs in comparison with NFs are their glycolytic metabolism and over-expression of alpha-SMA transcriptomes (Chen et al. 2017).

Here we used a label-free and real-time method to find lesions with high glycolytic behavior in their live states for analysis and investigate their specifications. The technique (called a cancer diagnostic probe (CDP)) has been based on electrochemical tracking of ROS/H_2O_2 released from the preneoplastic/neoplastic cells in the cavity side margins ((Miripour et al. 2022a, b; Dabbagh et al. 2021), US 11,179,076 B2, US 10,786,188 B1, US 11,179,077 B2, US 11,181,499 B2). The indicated levels of released ROS/H_2O_2 in pathologically free margins may correlate with CAF accumulations and the occurrence of field cancerization (Supplementary Section 1). This could be of significant impact to be further investigated. Finding and dissecting such CAFs may include valuable data about their phenotype and potential role in inducing neoplastic changes in epithelial cells, which were experimentally studied in this article.

We derived fibroblasts from the dissected specimens of 33 breast cancer mastectomy cases without inducing any perturbation or bias in the surgery and pathology trends. The specimen was dissected from the lesions, which weren't important for pathological evaluation. The CDP score of each specimen was recorded, and a part of the specimen was used for H&E and PCR evaluation to find any correlation between the presence and activity of CAFs, levels of expressed cancer-associated transcriptomes, and the presence/absence of cancer cells in the specimen. Also, CAFs interacted with breast non-cancer (MCF10-A) and cancer (MCF-7) cell lines, and the co-effects of CAFs and breast cell lines on each other were evaluated. We aimed to find a relation between levels of ROS/H_2O_2 released through the glycolysis metabolism of CAFs and the induced cancerous transformation transcriptomes in adjacent epithelial cells through molecular analysis.

We found that CAFs just could be actively found in adjacent cancer cells. Hence, we may not have active CAFs in the absence of cancer/pre-cancer cells except just adjacent to them (to promote their MCT4 pathway). This may be a new hallmark to understand better the hidden factors behind the local recurrence of breast cancer.

Material and methods

CDP structure and protocols

CDP is a cancer diagnostic probe that can diagnose the presence of pre-neoplastic/neoplastic cells in either cavity side margins of the patient's tumor during breast cancer surgery. It consists of an integrated automatic electrochemical readout board and a sensing disposable head probe as the main diagnostic part of the system. The sensing head probe was fabricated by the growth of Multi-Walled Carbon Nanotubes (MWCNTs) on the tip of steel needles in the conformation of three electrodes, named Working (WE), Counter (CE), and Reference (RE), with a triangular distance of 3mm from each other. The entered length of the needles into the breast margins is 4mm in the case of breast cancer surgery as the surgeons want to ensure the absence of any atypical/neoplastic or satellite lesions cells up to the depth of 4mm in the body side. The head probe is single-used and was sterilized under plasma sterilizer protocol (standard No: ISO/NP 22441) which didn't induce any perturbations on the morphology and function of the nanostructures.

The system determines lively the trace of ROS/H_2O_2 released from cancer or atypical cells, through reverse Warburg effect and hypoxia-assisted glycolysis pathways, in a quantitative electrochemical manner. A matched clinical diagnostic categorization between the pathological results of the tested tissues and response peaks of CDP was proposed based on pathological classification (ductal intraepithelial neoplasia (DIN), lobular intraepithelial neoplasia (LIN), and fibroepithelial lesion (FEL)) with the latest reported modifications. Still, no intra-operative technique has been reported for the detection of cavity

side surgical margins with pathologically approved classification in breast cancer (as one of the most important one-surgeries required for accurate margin detection).

During the lumpectomy or mastectomy surgery, the CDP was used for checking both cavity side margins to observe any probable matching between the suggested pathological classification of CDP scores and the final diagnostics of the samples declared by pathologists. At first, Sterilized CDP (stored in ambient exposed to a formalin tablet for one day) was turned on and connected to the software. Then the head probe (sterilized by plasma standard protocol) was connected to the CDP and the body side margins of the patient undergone tumor dissection were checked by CDP. After tumor dissection, all of the regions in the body side margins were tested by CDP (Superior, inferior, medial, lateral, superficial, and deep). Depending on the size of the tumor and its proximity to one of the margins (not all of the margins), some margins must undergo further analysis. In this regard, the internal regions with more joint boundaries with the tumors would require further scans due to their larger formed internal margins. If a region is positively scored by CDP, its neighbors (with a width of 3mm) and under-existed margin should also be checked by CDP. As a result, surgeons could excise the involved region with safe neighbors. The gold standard is permanent H&E/IHC assay ((Miripour et al. 2022a, b; Dabbagh et al. 2021), US 11,179,076 B2, US 10,786,188 B1, US 11,179,077 B2, US 11,181,499 B2).

Isolation of human breast fibroblasts and cell culture

Breast tissues with evaluated glycolytic behavior were obtained from the dissected specimens of 33 breast cancer mastectomy cases without inducing any perturbation or bias in the surgery trend. Also, a breast sample from mammoplasty surgery was used as a negative control for PCR analysis. Fibroblasts were isolated from these dissected breast regions. Tissues containing the CAFs were placed in collagenase type I (1 mg/mL; Boehringer Mannheim) and hyaluronidase (125 units/mL; Sigma-Aldrich) at 37 °C with agitation for 12–18 h. in Dulbecco's modified Eagle's medium (DMEM) with 10% fetal bovine serum (FBS) and placed on a shaker within the cell culture incubator until tissues were dissociated. Following this, a cell strainer was used to isolate cells from the dissociated tissues and re-suspended in complete DMEM. Then it was centrifuged at 4000 rpm for 3 min, and the pellet was resuspended in DMEM with 10% FBS and then expanded into a cell culture plate with 48 wells and stored up to passage 3 to population doublings within the total of 8–10 days after tissue dissociation (Truong et al. 2019; Orimo et al. 2005).

ROS assay

ROS generation was analyzed with a CM-H2DCFDA assay. This probe is converted to DCF with a green fluorescent property by esterase enzymes in the cytosol of the cells. To do this experiment, after culturing the Fibroblast cultured cells overnight, the cells are washed twice with PBS, and then 500 µL of the CM-H2DCFDA solution with a concentration of 20 µM is added. After 30 min incubation at room temperature and dark, cells are washed and imaged with a fluorescent microscope. As a negative control, a sample of cells was incubated with 12 mg NAC (N-Acetyl Cysteine) as a ROS scavenger and then treated with CM-H2DCFDA. The samples were imaged with a fluorescent microscopy system (Miripour et al. 2022a).

immunohistochemical staining procedure

The resected surgical tissue slides were deparaffinized in xylene, hydrated in dilutions of alcohol series, and immersed in 0.3% hydrogen peroxide in methanol to suppress endogenous peroxidase activity. TE buffer (10 mM Tris and 1 mM EDTA, pH 9.3) was used to treat sections at 98ºC for 30 min. Each section was blocked with 0.1% Tween 20 in PBS containing 4% bovine serum albumin for 30 min to reduce non-specific staining. The sections were incubated with anti-SMA (1:100, Millipore, Billerica, MA, USA) in PBST containing 3 mg/ml goat globulin (Sigma, St. Louis, MO, USA) for 60 min at room temperature, followed by three subsequent washes with buffer. Sections were then incubated with an anti-mouse/rabbit antibody (Envision plus, Dako) for 30 min. The chromogen used was 3,39-diaminobenzidine. Meyer's hematoxylin was used to counterstain the sections. Negative controls for immunostaining were obtained by excluding the primary antibody (Ha et al. 2014).

Quantitative real-time polymerase chain reaction (qRT-PCR)

The total RNA of breast dissected samples was extracted using an RNX kit (Sinaclon, Iran) according to the manufacturer's protocol. For each sample, 1 µg of RNA was reverse transcribed into complementary DNA (cDNA) using a cDNA synthesis Kit (Anacell, Iran) and analyzed with a StepOne real-time PCR system (Applied Biosystems) applying an SYBR Green PCR Master Mix (Anacell, Iran) to evaluate the gene expression of Glut-1, MMP-2, N-Cadherin, MMP-9. Sets of primers specific to each gene are provided in Supplementary Table 1. The human beta-actin (h-ACTB) gene was used to normalize the mRNA expression level of

each gene. Also, data analysis was carried out based on the $2^{-\Delta\Delta CT}$ method.

Twenty-eight samples with high glycolytic behavior and histologically negative were compared to the min value of the positive and max value of negative controls. Also, all samples were normalized to the mammoplasty sample.

Cell image analysis

ImageJ software and the OpenCV python library were used for cell detection and labeling through image processing tools. Each image was analyzed using various cell detection techniques to find the most applicable one. Shape, size, and circularity were considered parameters to distinguish between different cell lines in an identical image. Analysis was repeated separately for each different cell line present in an image and based on its particular parameters. Then, the results were shown simultaneously in the original image.

Statistical analysis

Data on bar graphs are expressed as means ± SD or ± SEM (as indicated). Statistical analysis was performed using one-way ANOVA, followed by Tukey's multiple comparisons test for repeated measurements, with the significance assessed at the 5% significance level ($P < 0.05$).

Results

CAFs are activated fibroblasts with heterogeneous shapes and metabolism within the tumor microenvironment and adjacent to the tumor boundaries (Ping et al. 2021). They secret various factors that play key roles in tumor development, metastasis, and resistance to therapy (Gadaleta et al. 2022; Orimo et al. 2005; Ping et al. 2021) (Fig. 1).

We investigated the hypoxia glycolysis behavior of tumor central and margin sides of breast cancer patients who had undergone mastectomy by CDP as a known glycolysis probing system by presenting the level of ROS-associated electrochemical peaks (Miripour et al. 2022a, b; Dabbagh, et al. 2021). Our gold standard for the pathological state of the specimen was H&E staining and diagnosis by pathologists.

Fibroblasts from the dissected specimens of 33 breast cancer mastectomy cases (which weren't important for pathological evaluation) were investigated. The CDP score for the ROS level of each lesion was recorded before dissection. We pathologically and biologically analyzed these fibroblasts to understand if they are CAFs or NFs. A part of the specimen was used for H&E and PCR evaluation to find any correlation between the presence and activity of CAFs, levels of expressed cancer-associated

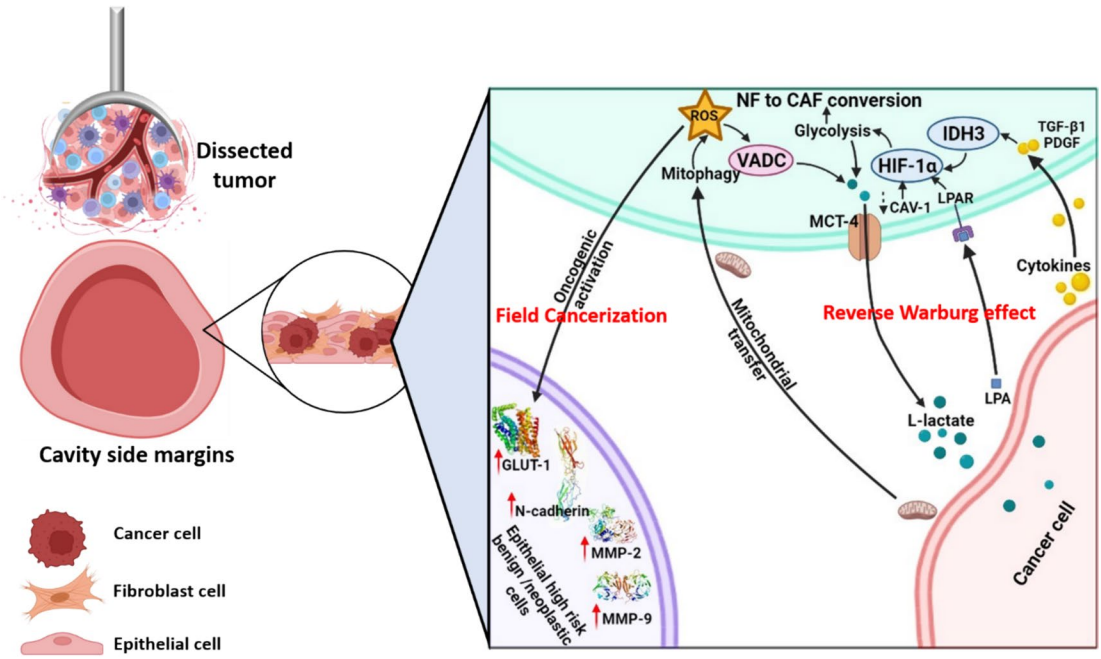

Fig. 1 The schematic of field cancerization procedure in the tumor microenvironment. Hydrogen peroxide released by tumor cells promotes oxidative stress to surrounding stromal cells, such as fibroblasts. Additionally, oxidative stress in fibroblasts leads to ROS production in the tumor stroma, allowing cancer cells to mutate further, eventually resulting in stromal lactate production and metastasis. Furthermore, hydrogen peroxide and ROS production can also mutagenize adjacent normal epithelial cells, promoting the growth of new cancerous cells (Lisanti et al. 2011)

transcriptomes, electrochemical levels of released ROS from the lesion, and the presence or absence of cancer cells in the specimen. Also, extracted fibroblast cells were exposed individually near breast non-cancer and cancer cell lines to investigate their effects on the invasion behavior of breast cells. The gold standard in this study was permanent pathology. Samples with high glycolytic behavior (due to CDP results) and positive for cancer in histology diagnosis were selected as positive controls (ID 3–5). These samples were IDC grade 2, High/Intermediate grade Ductal Carcinoma Insitu (DIN3,2). Samples with low glycolytic behavior and non-cancerous histology diagnosis (Non-proliferating FCC, Fatty breast tissue) were used as negative controls ID 1, 2, and mammoplasty operation samples. The other margin samples were histologically negative while showing high glycolytic behavior (based on CDP results). Through this investigation, we aimed to find a relation between levels of ROS/H_2O_2 released by the glycolytic cells (recorded by CDP) and the potential for cancerous transformation in these cells by evaluating their RT-PCR/IHC and fibroblast activity.

CAFs enhanced the aggressive behavior of cancer cells

First, 33 samples from individual patients underwent a mastectomy, excised, and driven by the protocol discussed in the method section to separate fibroblasts from other cells (immune, epithelial cells, endothelial cells, and so on) and recultured individually. The protocol for investigating the behavior of extracted fibroblasts from dissected tissues is presented in Fig. 2.

Alpha-SMA is a specific IHC marker for distinguishing CAFs from NFs (Ha et al. 2014). The tissue sample with ID 4, which had high glycolytic behavior and positive histological diagnosis (High-grade Ductal Carcinoma (DIN 3)), showed a positive expression of alpha-SMA IHC (Fig. 3a). Also, fibroblast cells excised and cultured from this sample showed positive staining for alpha SMA ICC (Fig. 3b) and negative staining for the epithelial marker E-cadherin (Fig. 3e). However, fibroblast cells driven from non-cancer breast tissue (ID 2: fatty breast tissue) with low glycolytic behavior showed negative staining for IHC and ICC of alpha SMA (Fig. 3b,d).

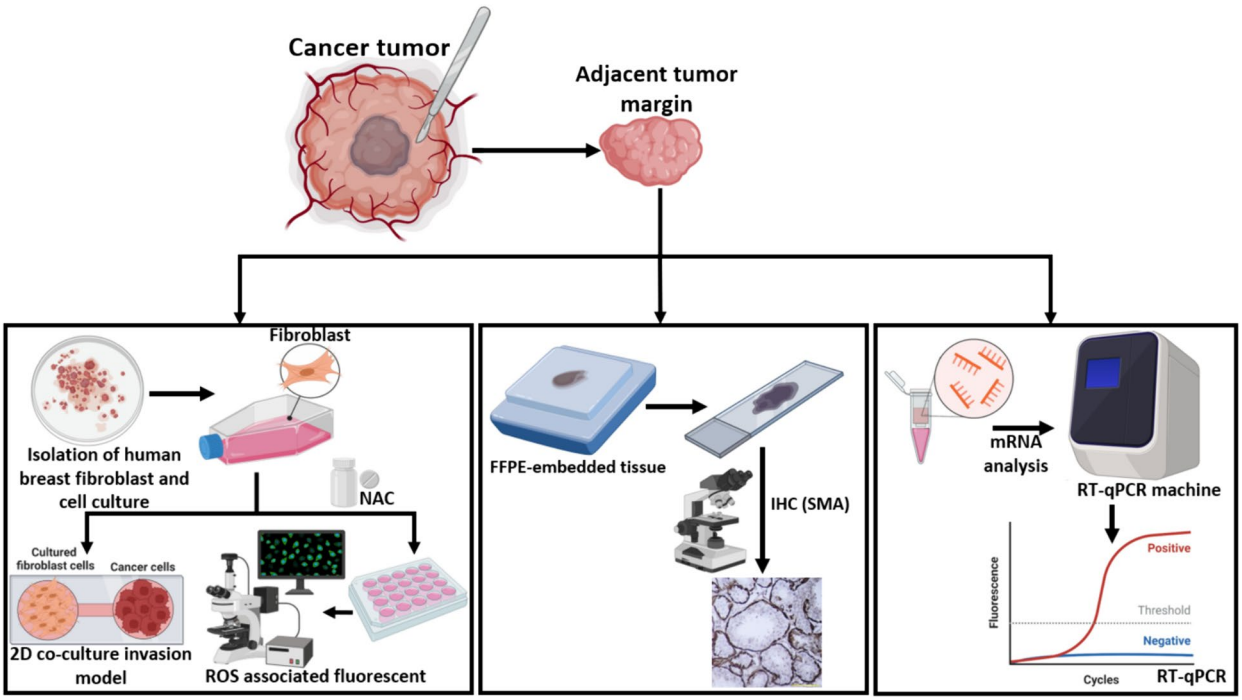

Fig. 2 The protocol for investigating CAFs in dissected tissues from breast cancer patients. The specimen was dissected from the lesions, which were not essential for pathological evaluation. In order to find a correlation between the presence and activity of CAFs, the levels of expressed cancer-associated transcriptomes, and the presence or absence of cancer cells in the specimen, the CDP score of each specimen was recorded, and a portion of each specimen was used for H&E and PCR evaluation. Moreover, CAFs interacted with breast non-cancer (MCF10-A) and cancer (MCF-7) cell lines, and their interactions were evaluated. Molecular analysis was performed to discover a relation between ROS/H2O2 levels released by CAFs through glycolysis metabolism and transcriptomes of adjacent epithelial cells that undergo cancerous transformation

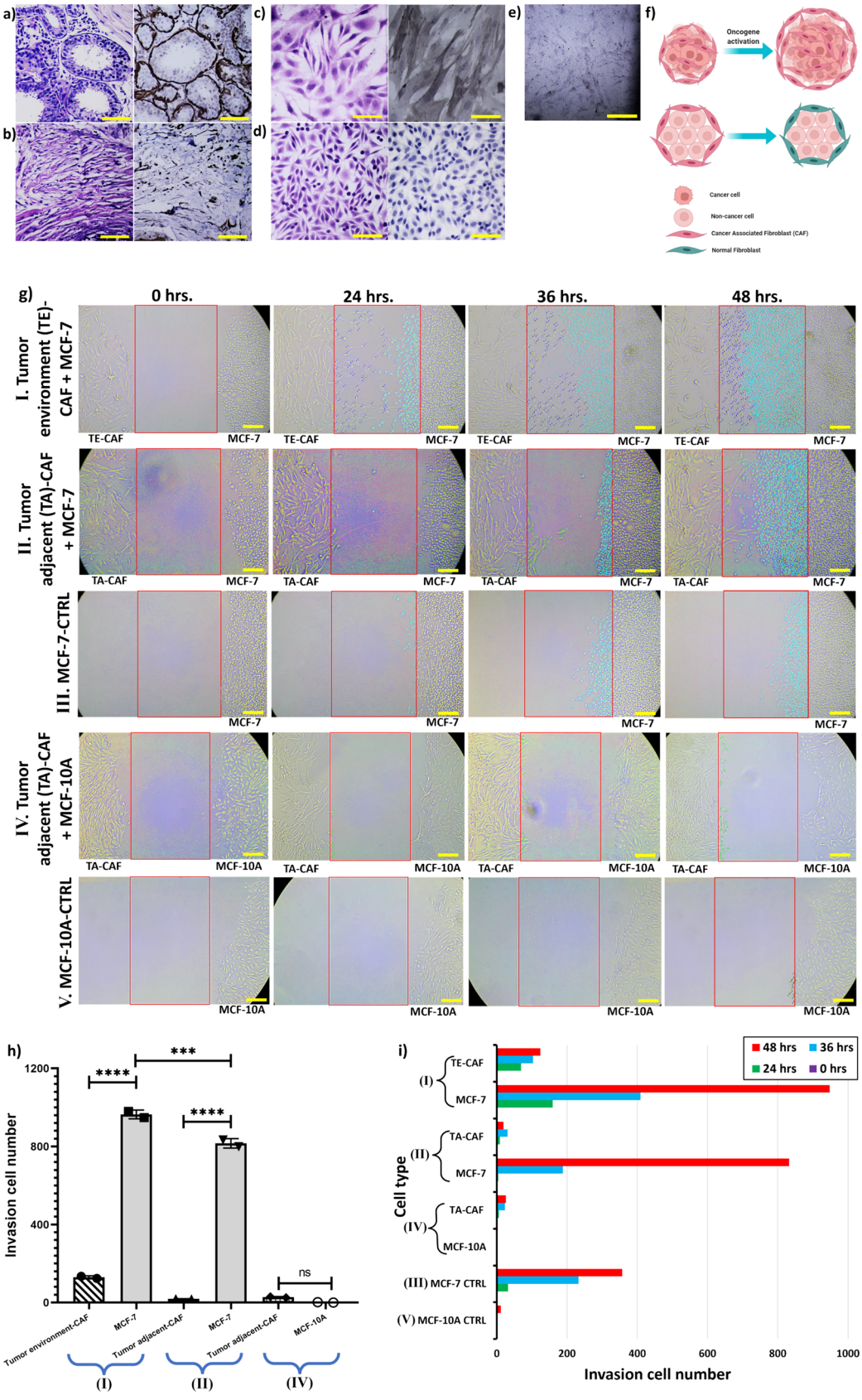
a)
b)
c)
d)
e)
f)
Oncogene activation
Cancer cell
Non-cancer cell
Cancer Associated Fibroblast (CAF)
Normal Fibroblast
g)
0 hrs.
24 hrs.
36 hrs.
48 hrs.
I. Tumor environment (TE)-CAF + MCF-7
II. Tumor adjacent (TA)-CAF + MCF-7
III. MCF-7-CTRL
IV. Tumor adjacent (TA)-CAF + MCF-10A
V. MCF-10A-CTRL
TE-CAF
TA-CAF
MCF-7
MCF-10A
h)
Invasion cell number
1200
800
400
0
****
***
****
ns
Tumor environment-CAF
MCF-7
Tumor adjacent-CAF
MCF-7
Tumor adjacent-CAF
MCF-10A
(I)
(II)
(IV)
i)
48 hrs
36 hrs
24 hrs
0 hrs
Cell type
(I) TE-CAF
MCF-7
(II) TA-CAF
MCF-7
(IV) TA-CAF
MCF-10A
(III) MCF-7 CTRL
(V) MCF-10A CTRL
0
200
400
600
800
1000
Invasion cell number

◂**Fig. 3** H&E staining and SMA IHC marker expression of paraffin-embedded of **a** sample ID 4, which had high glycolytic behavior and positive histological diagnosis (high-grade ductal carcinoma (DIN 3), and **b** sample ID 2 with low glycolytic behavior and negative histological diagnosis (fatty breast tissue), H&E staining and SMA marker of isolated CAFs from samples **c** ID 4, and **d** ID 2, **e** Epithelial marker E-cadherin of CAF. All the primary cultured CAFs expressed SMA highly (Ha et al. 2014) but did not express E-cadherin, presenting characteristics of CAFs (Yu et al. 2014). **f** Schematic of CAF behavior in adjacent tumoral and non-tumoral cells. **g** Evaluating fibroblast cells behavior extracted from the samples ID 4, 2 tissues and cultured in interaction with non-cancerous (MCF-10A) and cancerous (MCF-7) breast cells, tumor environment (TE)-CAF, tumor-adjacent (TA)-CAF. **h** Cell invasion ability was measured in three groups. The invasion ability of the MCF-7 cell lines cultured with tumor environment and adjacent CAF was significantly greater than MCF-10A non-cancer cells ($P < 0.0001$). **i** The exact invasion number of cells to the channel for each group. Each bar is equal to 100 µm

To evaluate the effect of CAF interactions with cancer and non-cancer cells in the tumor microenvironment, fibroblast cells extracted from breast margin tissues with high glycolytic behaviors were exposed to them. IHC and ICC analyses showed expression of alpha SMA and non-expression of E-Cadherin on these cells (Fig. 3a, c, e), which indicates the CAF nature of these cells. Some of these cells were extracted from breast lesions that were histologically negative for cancer, and others were extracted from histologically positive lesions (Fig. 3a, b). The similar specification of these cells is high glycolytic levels of their primary lesion and IHC/ICC expressing in favor of being CAFs. The mentioned fibroblasts were individually exposed to breast cancer (MCF-7) and non-cancerous (MCF-10A) cell lines. It was observed that MCF-7 cells showed a significant increase in their proliferation after being exposed to CAFs, (either to tumor environment (TE)-CAF (Fig. 3g (I)) or tumor adjacent (TA)-CAF (Fig. 3g (II)). About 948 and 833 MCF-7 cells invade the joint channel (between CAFs and breast cells culturing well (Fig. 3h, i)) after exposure to tumor environment (TE)-CAF and tumor-adjacent (TA)-CAF, respectively. But just 357 MCF-7 cells come to the channel in the control group (without exposure to the CAF). Also, the CAFs showed hyperactivated proliferation and extension in interaction with breast cancer cells (Fig. 3g–i).

On the other hand, it was observed that CAF's hyperactive behavior regressed when they were exposed to non-cancerous breast cells (MCF-10A) (Fig. 3g (IV)). Also, no hyperproliferation behavior was observed in the non-cancer breast cells after being interacted with CAFs (tumor adjacent (TA)-CAF, which was extracted from histologically non-cancer lesions with high glycolytic behavior (Fig. 3g (IV)).

So it seems that CAFs and MCF-7 show synergic proliferative behavior in their co-interactions. While CAFs and MCF-10A not only showed no synergic proliferation but also CAFs showed regressed activity in interaction with MCF10A cells (Fig. 3g–i).

CAFs promote ROS expression of cancer cells

NAC ((*N*-acetyl-L-cysteine) is a ROS Inhibitor (ab143032)) agent used in cellular investigations (Halasi et al. 2013; Zhang et al. 2011), and medical purposes (Shi and Puyo 2020; Sengupta and Dutta 2022). Here, it was used to evaluate ROS/hypoxic functions of fibroblasts before and after exposure near the breast cancer cell line (MCF-7). We also evaluated the electrochemical level of ROS/H_2O_2 in those cell cultures. In this regard, 1 µL (12 mg) of NAC was individually added to the CAFs cultured samples, and their ROS electrochemical peak was recorded in time intervals of two hours up to 8 h. The fluorescent microscope images of negative control (without NAC) after 8 h of adding NAC and positive control (100µM of H_2O_2) to breast cancer cell line (MCF-7), tumor environment CAF, tumor-adjacent CAF, and co-culture of MCF-7 + tumor environment CAF/tumor adjacent CAF were presented in Fig. 4a. ROS fluorescent assay (see method section) showed a drastic reduction in the expression of green fluorescent protein by samples including CAFs, MCF-7, and their co-interaction after treatment with 1µl of NAC (Fig. 4a). Similarly, a sharp reduction in ROS electrochemical peaks was observed in all mentioned samples (Fig. 4b).

RT-PCR and immunohistochemistry analysis of glycolytic breast cells

It is believed that high-level expression of glucose transporter-1 (GLUT1) transcriptome, as the main indication of glycolysis metabolism, is found in several types of cancer, including breast cancer, and is associated with poor survival rates (Kunkel et al. 2003; Kang et al. 2002). Glut1 facilitates glycolytic phenotypes such as glucose uptake, cellular ATP, and lactate production levels for cancer cells (Oh et al. 2017). The matrix metalloproteinases (MMPs) transcriptomes are a family of zinc-dependent proteases. MMP-2 and MMP-9 are critical representatives of the MMP family and have been demonstrated to be important factors in promoting tumor invasion and metastasis by degrading extracellular matrices (Iochmann et al. 2009; Safranek et al. 2009). According to many studies, MMP-2 and MMP-9 are highly expressed in breast cancer tissues and are closely associated with lymph node metastasis and tumor staging.

Moreover, N-cadherin-1 is another significant transcriptome activated during cancer. N-cadherin is a member of classical cadherins' calcium-dependent adhesion molecule family, directly mediating homotypic and heterotypic cell–cell adhesion (Mrozik et al. 2018). N-cadherin expression is aberrant in many solid tumors, indicating epithelial-to-mesenchymal transition, leading to the development of aggressive tumors (Cao et al. 2019). Several mechanisms have been identified in which N-cadherin

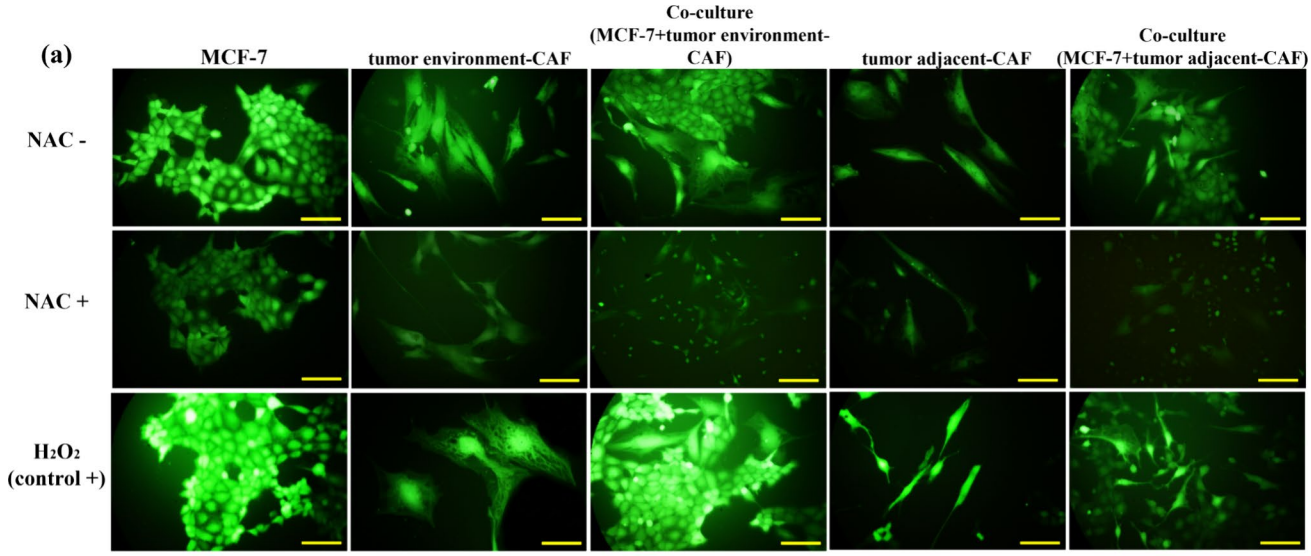

(b)

ROS related electrochemical current peak (μA)	Control (no NAC)	Cells treated with NAC after 2 hrs.	Cells treated with NAC after 4 hrs.	Cells treated with NAC after 8 hrs.
MCF-7	1003.3	741.6	523.5	145.4
Tumor environment-CAF	872.4	654.3	440.6	87.2
MCF-7 +tumor environment-CAF	1570.4	828.8	545.3	161.6
Tumor adjacent-CAF	748.5	598.2	335.5	98.8
MCF-7 +tumor adjacent-CAF	1256.7	750.8	395.26	188.5

Fig. 4 **a** The fluorescent microscope images of negative control (without NAC) after 8 h of adding NAC and positive control (100μM of H_2O_2) to breast cancer cell line (MCF-7), tumor environment CAF, tumor-adjacent CAF, and co-culture of MCF-7 + tumor environment CAF/tumor adjacent CAF, **b** electrochemical current peaks of control (without NAC), and the cells treated with NAC after 2, 4, 6, and 8 h. Each bar is equal to 100 μm

promotes tumor cell migration: enhancing Fibroblast growth factor receptor-1 (FGFR-1) signaling, modulating canonical Wnt signaling, and facilitating collective cell migration (Mrozik et al. 2018).

RT-PCR results of the GLUT-1, MMP 2, MMP-9, and N-cadherin expression in breast tissues of the studied cases are presented in Fig. 5. It shows meaningful oncogenic changes of about 18.5% (MMP 2, MMP-9, and N-cadherin) in tissues with non-cancerous histology but high glycolytic behavior (ID 8–10, 28, 30–33) with respect to negative controls (ID 1,2). The number of samples with cancer-associated transcriptomic expression (GLUT-1, MMP 2, MMP-9, and N-cadherin) which have more than the mean value expression of positive control samples (histologically cancerous samples; ID 3–5) were about 40.7%, 18.5%, 18.5%, and 18.5%. At mean 70.4%, 66.7%, 70.4%, and 44.5% increments were observed in GLUT-1, MMP-2, N-cadherin, and MMP-9 transcriptomes by highly glycolytic but histologically cancer-free expression samples in comparison with negative controls (histologically non-cancer lesions with low glycolytic behavior).

Moreover, IHC analysis for cancer-associated markers (VEGF, MMP-2, N-Cadherin, and MMP-9) (Kim et al. 2016) was conducted on the samples. None of them was expressed in negative controls. In positive control samples, there was a considerable expression of VEGF, MMP-2, N-Cadherin, and MMP-9. In samples with positive scores of CDP and negative diagnosis of histology, such expressions were 83%, 39%, 0%, and 61% of samples have proportion and intensity ≥ 1, respectively.

Discussion

We investigated the cancer-associated behaviors of the lesions adjacent to tumor margins and found two critical factors about biologically high-risk while histologically benign representations in some of such lesions, which was

a)

Variable	Patients (N=33)
Age	43.5 (30-65)
Sex	
Female	33 (100%)
Tumor Type	
IDC	31 (88%)
ILC	2 (6%)
Tumor Size (min-max)	1/5-6 cm
Tumor Location	
upper-outer quadrant (UOQ)	18 (58%)
upper-inner quadrant (UIQ)	3 (10%)
lower-outer quadrant (LOQ)	9 (29%)
lower-inner quadrant (LIQ) nipple and central breast	1 (3%)
Tumor Site	
Left breast	23 (70%)
Right breast	10 (30%)
Type of surgery	
Lumpectomy	0 (0%)
Mammoplasty	33 (100%)
State of patients	
Surgery after Neoadjuvant	1 (3%)
First surgery	32 (97%)

b)

Patient ID	Margin Type	Hypoxia Glycolysis related electrochemical current peak (μA)	CDP declaration	Pathological Diagnosis
1	Superolateral	77	Neg.	Non proliferating FCC
2	Lateral	59	Neg.	Fatty breast tissue
3	Inferior	490	Pos.	IDC grade 2
4	Inferior	850	Pos.	High grade Ductal Carcinoma Insitu (DIN3) synonym of comedo carcinoma, ductal intraepithelial neoplasia (DIN2) synonym of intermediate grade of Ductal carcinoma insitu, a small focus suspicious for invasive carcinoma with severe lymphocytic infiltrative
5	Medial	616	Pos.	IDC Nuclear grade 2 , Ductal invasive neoplasia (DIN3) suggestive of high grade ductal carcinoma insitu
6	Superior	434	Sus.	FCC with CCC and CCH
7	Medial	358	Sus.	AVN, FCC, moderate typical ductal hyperplasia
8	Inferior	428	Sus.	FCC with CCC, florid typical ductal hyperplasia
9	Medial	381	Sus.	Non proliferating FCC with apocrine metaplasia
10	Inferior	453	Sus.	FCC with columnar cell change and apocrine metaplasia/A focus of florid typical ductal hyperplasia is also seen/Numerous promotion nuclei with lobular cells are seen
11	Inferolateral	356	Sus.	FCC with moderate usual ductal hyperplasia
12	Superolateral	394	Sus.	FCC with CCC
13	Lateral	406	Sus.	FCC with CCC
14	Inferior	376	Sus.	FCC with CCC
15	Medial	460	Sus.	FCC with CCC and CCH, Florid typical ductal hyperplasia, Sclerosing adenosis
16	Lateral	420	Sus.	FCC with focal tubular adenosis, Macrocalcification are also seen, FCC with apocrine metaplasia, FCC with CCC and CCH
17	Inferior	380	Sus.	FCC with moderate typical ductal hyperplasia, CCC are also seen.
18	Superomedial	385	Sus.	FCC with CCC
19	Medial	352	Sus.	Fibrocystic change with mild usual ductal hyperplasia
20	Inferior	400	Sus.	FCC with CCC
21	Medial	389	Sus.	CCC
22	Medial	442	Sus.	FCC with CCC and CCH
23	Medial	352	Sus.	FCC
24	Medial	375	Sus.	FCC with CCC
25	Superior	372	Sus.	Non Proliferating FCC with apocrine metaplasia
26	Medial	366	Sus.	Proliferative fibrocystic change with mild to moderate usual ductal hyperplasia without atypia, stromal adenosis and fibrosis seen
27	Medial	387	Sus.	FCC with blunt duct adenosis, Columnar cell changes are also seen.
28	Inferior	383	Sus.	FCC with CCC
29	Medial	391	Sus.	Non proliferating FCC with apocrine metaplasia
30 (Neoadjuvant)	Inferior	399	Sus.	FCC with CCC
31	Medial	461	Sus.	FCC with CCC, CCH, papillary lesion with apocrine metaplasia , florid ductal hyperplasia
32	Inferolateral	381	Sus.	FCC with CCC, microcalcification are also seen
33	Inferomedial	375	Sus.	FCC with CCC

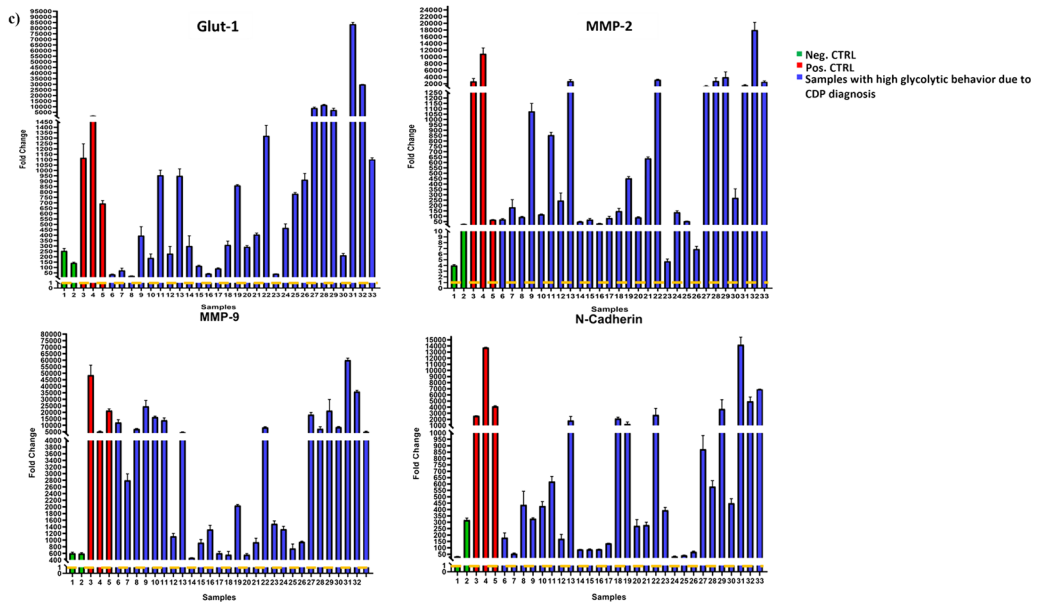

Fig. 5 **a** Clinical and pathologic characteristics of patients and adjacent tumor margins samples randomly assigned to this study, **b** CDP ROS/H_2O_2 current peaks and declaration and pathological diagnosis of samples, **c** RT-PCR of oncogenic associated transcriptomes adjacent tumor margins samples, all samples expression were normalized to mammoplasty expression value (Green and red color indicated negative and positive controls diagnosed by CDP and confirmed by pathology, and the blue ones are margin samples with high glycolytic behavior but histologically negative), **d** Heat maps representing four transcripts were investigated on 33 cavity margins of breast cancer patients, **e** The comparative outcomes of the adjacent cavity margins RNA sequencing results to the control samples, **f** IHC of four transcripts VEGF, MMP-2,9, and N-cadherin were investigated on assayed samples. Intensity Score (Score 0: no or weak staining, Score 1: mild staining, Score 2: moderate staining, Score 3: strong staining), Proportion score (Score 0: no or weak intensity, Score 1: < 10% of tumor with strong intensity (SI), Score 2: = 10% ≤ strong intensity < 1/3 of tumor, Score 3: 1/3 ≤ strong staining < 2/3 of tumor), **f** IHC analysis for cancer-associated markers (VEGF, MMP-2, N-cadherin, and MMP-9) on the samples, **g** IHC VEGF, MMP-2, N-cadherin, and MMP-9 in negative control samples (CDP negative and H&E negative), positive control samples (CDP positive and H&E positive), and CDP positive and H&E negative samples. Each bar is equal to 100 μm

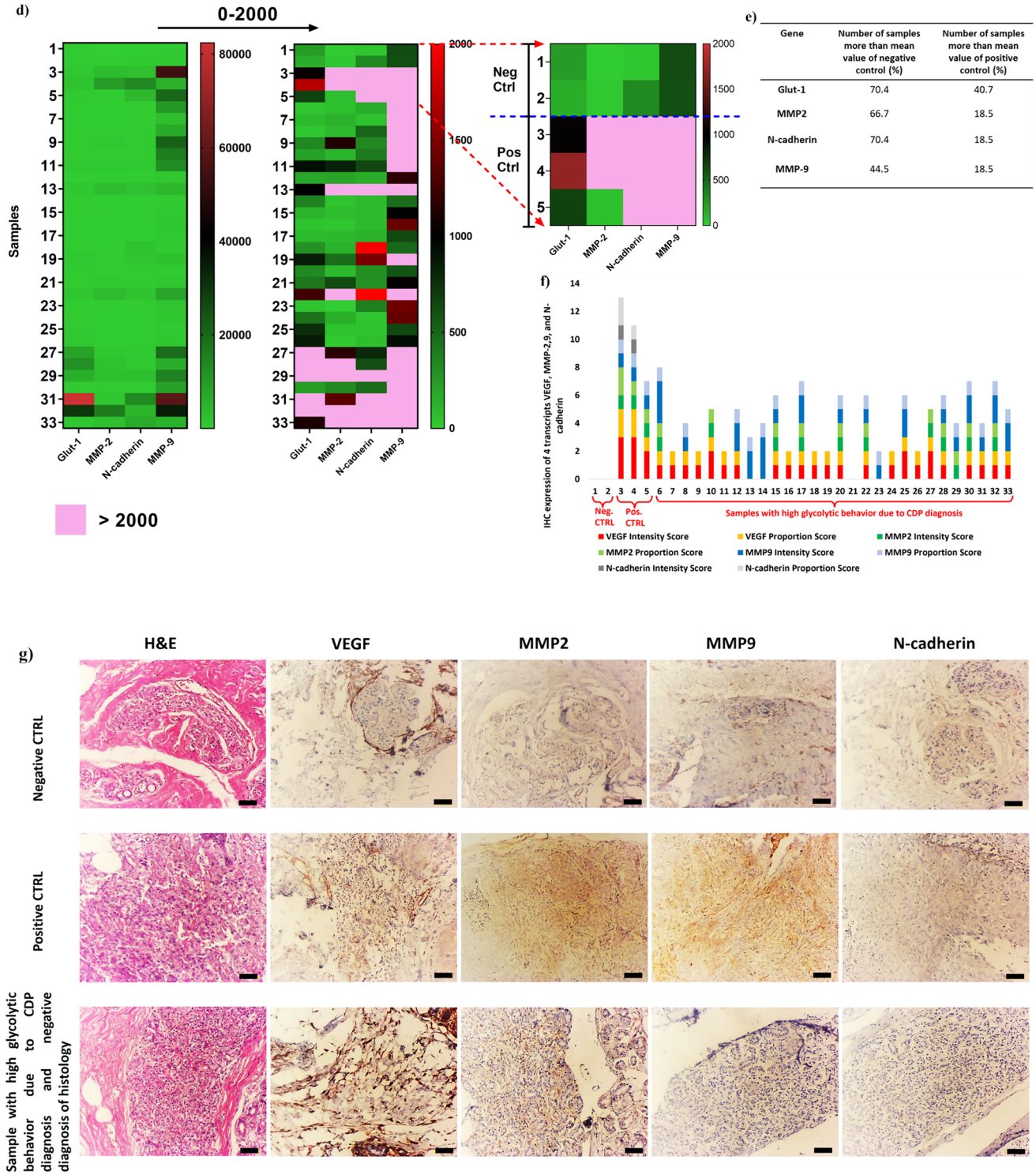

Fig. 5 (continued)

a strong correlation with their glycolytic metabolism; first: the expression of cancer transcriptomes such as GLUT-1, MMP-2, MMP-9, and N-cadherin in those lesions. Second the presence of active CAFs among epithelium which, due to our ex vivo observation, just become activated in the presence of cancer cells. Our main distinct factor in finding these lesions was the real-time electrochemical measuring of their released ROS levels with the assistance of a newly presented CDP system (Miripour et al. 2022a, b; Dabbagh et al. 2021). Also, florescent-based ROS detection was

applied to confirm the increased released ROS from those lesions to normal negative controls. It is known that preneoplastic and neoplastic breast cells (in adjacent margins) and their surrounding CAFs can increase their metabolism by switching to aerobic glycolysis [through Warburg, reverse Warburg and field cancerization effects (Potter et al. 2016; Chai and Brown 2009)], which results in the release of ROS by the cells in the intercoastal fluid. So, due to the correlation between ROS electrochemical expressed responses and florescent ROS release assay, the presence of CAFs could be a hallmark of oncogenic changes due to glycolytic-based ROS expression.

As shown in Figs. 3a–e, CAF (All the primary cultured CAFs express high levels of alpha SMA (Ha et al. 2014) while they do not express E-cadherin [as a molecular characteristic of CAFs) (Yu et al. 2014)] interaction by the non-cancer and cancer breast cells (Fig. 3g) demonstrates that the activation of the CAFs just could be happened in the presence of neoplastic cells. It was interesting that MCF-10A cells in the proximity of CAFs do not show any change in their growth, but the behavior of CAFs regresses. We observed that if there is a high ROS signal in a cavity margin with no observable cancer cells except CAFs (due to conventional histopathological assay), this margin should be further investigated because some single cancer or high risk precancer cells maybe existed in the vicinity of CAF (Fig. 3g–i), which causes oncogenic changes in cavity margin's fibroblasts. Presence of these CAFs may be due to he presence of such single cells. It means that CAFs without the presence of neoplastic cells in their neighbor area might not keep their function. So, if a distribution of CAFs were found in breast lesions, there may be a hallmark about presence of scattered single preneoplastic or cancer cells in that lesion even if they were observed in histological slide. Activated cancer-associated proteins observed in those lesions (Fig. 5f–g) were in accordance to this hypothesis.

RT-PCR of those lesions also showed meaningful increased expression of cancer-associated transcriptomes (MMP-2, MMP-9, N-cadherin) and glycolytic metabolism (GLUT-1) in those cells with respect to histologically benign and metabolically non-glycolytic cells (negative controls) (Fig. 5). Also, oncogenic changes in GLUT-1 were higher in about 40.7% of samples with non-cancerous histology but high glycolytic behavior, like positive controls. As it was predictable, the expression of the transcriptomes was much higher in positive control samples (Fig. 5c–e). Beta-actin transcriptome (conventionally applied as Housekeeping) also showed increased expression in malignant samples, which indicates the test's reliability because we observe an increase in beta-actin transcriptome in malignant breast cancer cells.

Co-culturing these CAFs with non-neoplastic (MCF-10A) and neoplastic (MCF-7) cells of the same patients and monitoring the ROS/Hypoxic changes in the co-culture near evaluating metabolic changes of the cells are our future trends in this investigation**.**

No expression of important breast cancer-associated proteins (evaluated by IHC) such as VEGF, MMP-2, N-Cadherin, and MMP-9 were observed in negative control samples (CDP negative and H&E negative). The strong and somehow perfect expression of these proteins was observed in positive control samples (CDP positive and H&E positive). We observed meaningful expression of these proteins in CDP samples (CDP positive and H&E negative) (Fig. 5f). In 71% (20/28) of the samples, there was a mild expression of VEGF, while 11% (3/28) of the samples had a moderate expression of VEGF. 39% (11/28) of those samples had mildly expressed MMP-2 as a protease enzyme produced by progressive cancer cells (Yaqoob et al. 2020). Moreover, 29% (8/28), 25% (7/28), and 7% (2/28) of the mentioned samples had mild, moderate, and strong expression of MMP-9 as a protease indicator of primary cancer cells (Huang 2018). So, it can be deduced that the expression of cancerous functional proteins in the histologically normal/benign cells with glycolysis metabolism (detected by CDP) was meaningfully further than in normal/benign cells without any glycolytic metabolism (negatively scored by CDP).

The main findings of this paper are that the presence of CAFs in the cavity side margins indicates the existence of cancerous, precancerous, or oncologically activated epithelial cells around CAFs. If these cells didn't exist in the margin lesions, CAFs would be downregulated, reducing their aggressive behaviors to normal fibroblasts. Hence, the presence of CAFs is correlated with the presence of high glycolytic metabolism in the lesion, high ROS level in the lesion, and finally aggressive cancer-associated proteins (such as MMP2, …) in the margin lesion while these metabolomes, molecules, and proteins are absent in the margins with negatively scored CDP response and low ROS level (Fig. 5). Other papers didn't report this result that CAFs could be down-functioned into behaviors similar to normal FBs if no cancer/precancer cells were in their adjacent, while this evidence was observed, discussed, and reported in our paper (Fig. 3). In summary, we concluded that: (1) High levels of ROS in the cavity side margins are correlated with the presence of cancer-associated fibroblasts (CAFs) near cancer or precancerous cells, or potentially activated to become cancer cells. (2) If none of these high-risk cells existed in the media, the CAFs would reduce their aggressive functions turned into normal FBs. (3) Similar to other papers we also observed the synergic effect of CAFs and breast cancer cells to each other due to secreting the by-products of glycolysis metabolism to the media. (4) CDP positively scored responses are important to be considered because even if no cancer cells were histologically found in the margin, high-risk epithelial cells in that margin express cancer-associated

proteins and metabolomes, which is one of the hallmarks that stimulate the fibroblast to become CAF. So, metabolic probing could be a good indicator to distinguish these cells.

Conclusion

In summary, we showed the hyperactivation of fibroblasts derived from cavity-side breast margins with glycolytic metabolism, even in the absence of neoplastic breast cells. These fibroblasts expressed CAF markers and RT-PCR of cancer-free margins with positive glycolytic metabolism and these CAFs, showed over-expression of cancer-associated transcriptomes, while the fibroblasts derived from cancer-free cavity side margins and absence of CAFs showed normal RT-PCR profile. At mean 70.4%, 66.7%, 70.4%, and 44.5% increments were observed in GLUT-1, MMP-2, N-Cadherin, and MMP-9 transcriptomes by highly glycolytic but histologically cancer-free expression samples in comparison with negative controls (histologically non-cancer lesions with low glycolytic behavior). Also, immunohistochemical analysis of important cancer-related proteins such as MMP-2, MMP-9, and VEGF revealed a significant presence of these proteins in glycolytic margins (with histology of non-cancerous lesions), while no expression of N-Cadherin was observed. Furthermore, cancer-free glycolytic margins contained CAFs capable of activating cancer cells in vitro. However, these CAFs were downregulated when interacting with normal breast cells. These pieces of evidence may present a hidden hallmark factor; the presence of CAFs in histologically cancer-free breast margins may warn about the presence of pre-cancer or cancer cells in a hidden state because CAFs could not be activated, and glycolytic function may not be traced in a cavity margin without any neoplastic/pre-neoplastic cells. Metabolic probing can provide valuable insights for more effective investigation of tumor margins in order to detect any oncogenic or oncoproteomic changes. This information can be crucial for improving the management of organ-conserving tumor surgery. The study results highlight the need for further research on non-histologically tumoral margins with glycolytic behavior and CAF content. This research may help in understanding the increased risk of cancerous changes in marginal cells.

Supplementary Information The online version contains supplementary material available at https://doi.org/10.1007/s00432-024-05943-8.

Acknowledgements We thank Professors Saeed Sarkar, Habib Mahmoudzadeh and S.R. Miri for their great scientific supports of this project.

Author contributions Zohreh Sadat Miripour manufactured the electrodes, designed a test setup for CDP clinical studies, performed most of the experiments, categorized the tabled data. Mina Aminifar, Farideh Makian, and Parisa Aghaee assisted in the isolation of human breast fibroblasts and cell culture preparation and also assisted in the experiment. Parisa Hoseinpour and Mohammad Parniani did the pathological experiments and declared the diagnosis. Fereshteh Abbasvandi and Mohammad Esmaeil Akbari supervised the clinical and surgical procedures and follow-ups. Koosha Karimi and Alireza Ghahremani performed material preparation, data collection, and assistance in the experiment. Mohammadreza Ghaderinia assisted in statistical analysis. Mohammad Abdolahad proposed the hypothesis of the paper, designed and coordinated the idea and all steps of the research, did the analysis and also wrote the manuscript. All authors commented on previous versions of the manuscript and approved the final manuscript for submission.

Funding This research was supported by the Iran Nano Fund institution, P.O. Box 1533984611, Tehran, Iran.

Availability of data and materials The authors declare that all the other data supporting the findings of this study are available within the article and its supplementary information files and from the corresponding author upon reasonable request. Also, the authors declare that all codes supporting the findings of this study are available from the corresponding author upon reasonable request. No datasets were generated or analysed during the current study.

Declarations

Conflict of interest The authors declare no competing interests.

Ethical approval and informed consent to participate Patients provided written informed consent according to an ethically approved protocol by the institutional review board of Tehran University of Medical Science (IR.TUMS.VCR.REC.1397.355) at our breast cancer central clinics and assistant hospitals for the use of their samples.

Consent for publication Not applicable.

Registration no. of the study Registry ID: IR.TUMS.VCR.REC.1397.355.

Animal studies Not applicable.

References

Cao Z-Q, Wang Z, Leng P (2019) Aberrant N-cadherin expression in cancer. Biomed Pharmacother 118:109320

Chai H, Brown RE (2009) Field effect in cancer-an update. Ann Clin Lab Sci 39(4):331–337
Chan JSK et al (2018) Cancer-associated fibroblasts enact field cancerization by promoting extratumoral oxidative stress. Cell Death Dis 8(1):e2562–e2562
Chen J et al (2017) Overexpression of α-sma-positive fibroblasts (CAFs) in nasopharyngeal carcinoma predicts poor prognosis. J Cancer 8(18):3897
Dabbagh N et al (2021) Accuracy of cancer diagnostic probe (CDP) for intra-surgical checking of cavity side margins in neoadjuvant breast cancer cases; a human model study. Int J Med Robot Comput Assist Surg 18:e2335
Erez N, Truitt M, Olson P, Hanahan D (2010) Cancer-associated fibroblasts are activated in incipient neoplasia to orchestrate tumor-promoting inflammation in an NF-κB-dependent manner. Cancer Cell 17(2):135–147
Gadaleta E, Thorn GJ, Ross-Adams H, Jones LJ, Chelala C (2022) Field cancerization in breast cancer. J Pathol 257:561–574
Gascard P, Tlsty TD (2016) Carcinoma-associated fibroblasts: orchestrating the composition of malignancy. Genes Dev 30(9):1002–1019
Giannoni E et al (2010) Reciprocal activation of prostate cancer cells and cancer-associated fibroblasts stimulates epithelial-mesenchymal transition and cancer stemness. Cancer Res 70(17):6945–6956
Ha SY, Yeo S-Y, Xuan Y, Kim S-H (2014) The prognostic significance of cancer-associated fibroblasts in esophageal squamous cell carcinoma. PLoS ONE 9(6):e99955
Halasi M, Wang M, Chavan TS, Gaponenko V, Hay N, Gartel AL (2013) ROS inhibitor *N*-acetyl-L-cysteine antagonizes the activity of proteasome inhibitors. Biochemical Journal 454(2):201–208
Huang H (2018) Matrix metalloproteinase-9 (MMP-9) as a cancer biomarker and MMP-9 biosensors: recent advances. Sensors 18(10):3249
Iochmann S et al (2009) Transient RNA silencing of tissue factor pathway inhibitor-2 modulates lung cancer cell invasion. Clin Exp Metastasis 26(5):457–467
Kang SS et al (2002) Clinical significance of glucose transporter 1 (GLUT1) expression in human breast carcinoma. Jpn J Cancer Res 93(10):1123–1128
Kim S-W, Roh J, Park C-S (2016) Immunohistochemistry for pathologists: protocols, pitfalls, and tips. J Pathol Transl Med 50(6):411
Kunkel M et al (2003) Overexpression of Glut-1 and increased glucose metabolism in tumors are associated with a poor prognosis in patients with oral squamous cell carcinoma. Cancer Interdiscip Int J Am Cancer Soc 97(4):1015–1024
Liao Z, Tan ZW, Zhu P, Tan NS (2018) Cancer-associated fibroblasts in tumor microenvironment–Accomplices in tumor malignancy. Cell Immunol 343:103729
Lisanti MP et al (2011) Hydrogen peroxide fuels aging, inflammation, cancer metabolism and metastasis: the seed and soil also needs "fertilizer." Cell Cycle 10(15):2440–2449
Louault K et al (2019) Interactions between cancer-associated fibroblasts and tumor cells promote MCL-1 dependency in estrogen receptor-positive breast cancers. Oncogene 38(17):3261
Martinez-Outschoorn UE et al (2010) Oxidative stress in cancer associated fibroblasts drives tumor-stroma co-evolution: a new paradigm for understanding tumor metabolism, the field effect and genomic instability in cancer cells. Cell Cycle 9(16):3276–3296
Miripour ZS et al (2022a) Electrochemical tracing of hypoxia glycolysis by carbon nanotube sensors, a new hallmark for intra-operative detection of suspicious margins to breast neoplasia. Bioeng Transl Med 7:e10236
Miripour ZS et al (2022b) Human study on cancer diagnostic probe (CDP) for real-time excising of breast positive cavity side margins based on tracing hypoxia glycolysis; checking diagnostic accuracy in non-neoadjuvant cases. Cancer Med 11(7):1630–1645
Mrozik KM, Blaschuk OW, Cheong CM, Zannettino ACW, Vandyke K (2018) N-cadherin in cancer metastasis, its emerging role in haematological malignancies and potential as a therapeutic target in cancer. BMC Cancer 18(1):1–16
Oh S, Kim H, Nam K, Shin I (2017) Glut1 promotes cell proliferation, migration and invasion by regulating epidermal growth factor receptor and integrin signaling in triple-negative breast cancer cells. BMB Rep 50(3):132
Orimo A et al (2005) Stromal fibroblasts present in invasive human breast carcinomas promote tumor growth and angiogenesis through elevated SDF-1/CXCL12 secretion. Cell 121(3):335–348
Ping Q et al (2021) Cancer-associated fibroblasts: overview, progress, challenges, and directions. Cancer Gene Ther 28(9):984–999
Potter M, Newport E, Morten KJ (2016) The Warburg effect: 80 years on. Biochem Soc Trans 44(5):1499–1505
Safranek J et al (2009) Expression of MMP-7, MMP-9, TIMP-1 and TIMP-2 mRNA in lung tissue of patients with non-small cell lung cancer (NSCLC) and benign pulmonary disease. Anticancer Res 29(7):2513–2517
Sengupta P, Dutta S (2022) *N*-Acetyl cysteine as a potential regulator of SARS-CoV-2-induced male reproductive disruptions. Middle East Fertil Soc J 27(1):1–6
Shi Z, Puyo CA (2020) *N*-Acetylcysteine to combat COVID-19: an evidence review. Ther Clin Risk Manag 16:1047
Truong D, Puleo J, Llave A, Mouneimne G, Kamm RD, Nikkhah M (2016) Breast cancer cell invasion into a three dimensional tumor-stroma microenvironment. Sci Rep 6:34094
Truong DD et al (2019) A human organotypic microfluidic tumor model permits investigation of the interplay between patient-derived fibroblasts and breast cancer cells. Cancer Res 79(12):3139–3151
Vanharanta S, Massagué J (2012) Field cancerization: something new under the sun. Cell 149(6):1179–1181
Yaqoob I, Saeed M, Azhar A (2020) MMP-2 levels evaluation and their relationship with breast cancer progression. Prof Med J 27(02):424–430
Yu Y, Xiao CH, Tan L, Wang QS, Li XQ, Feng YM (2014) Cancer-associated fibroblasts induce epithelial–mesenchymal transition of breast cancer cells through paracrine TGF-β signalling. Br J Cancer 110(3):724–732
Zhang F, Lau SS, Monks TJ (2011) The cytoprotective effect of *N*-acetyl-L-cysteine against ROS-induced cytotoxicity is independent of its ability to enhance glutathione synthesis. Toxicol Sci 120(1):87–97

Authors and Affiliations

Zohreh Sadat Miripour[1,2] · Mina Aminifar[1] · Parisa Hoseinpour[1,3] · Fereshteh Abbasvandi[4,5] · Koosha Karimi[1] · Alireza Ghahremani[1] · Mohammad Parniani[4] · Mohammadreza Ghaderinia[1] · Faride Makiyan[1] · Parisa Aghaee[1] · Mohammad Esmaeil Akbari[5] · Mohammad Abdolahad[1,2,6]

✉ Mohammad Abdolahad
m.abdolahad@ut.ac.ir; abdolahad@tums.ac.ir

[1] Nano Bio Electronic Devices Lab, Cancer Electronics Research Group, School of Electrical and Computer Engineering, College of Engineering, University of Tehran, P.O. Box 14395/515, Tehran, Iran

[2] UT&TUMS Cancer Electronics Research Center, University of Tehran, P.O. Box 14395/515, Tehran, Iran

[3] SEPAS Pathology Lab, P. O. Box 1991945391, Tehran, Iran

[4] ATMP Department, Breast Cancer Research Center, Motamed Cancer Institute, ACECR, P.O. Box 15179/64311, Tehran, Iran

[5] Cancer Research Center, Shahid Beheshti University of Medical Sciences, P.O. Box 15179/64311, Tehran, Iran

[6] Cancer Institute, Imam Khomeini Hospital, Tehran University of Medical Sciences, P.O. Box 1419733141, Tehran, Iran